J. Build. Mater. Struct. (2024) 11: 61-78 ***Original Article***
DOI: 10.34118/jbms.v11i1.3953

Experimental and Numerical Study of Mechanical Properties of Concrete Containing Biochar

Odeyemi S.O *, Adisa M.O, Olawale M.A, Abdulsalam A.O, Oloba J.A, Ibrahim H.A, Sanusi B.O, Eda J.O, Obisiji F.O

Department of Civil & Environmental Engineering, Kwara State University Malete, Nigeria
* Corresponding Author: samson.odeyemi@kwasu.edu.ng

Received: 18-01-2024 **Accepted: 15-06-2024**

Abstract. The production of cement is responsible for 7% of worldwide CO_2 emissions, leading to environmental threats and harm to ecosystems. Given the significant expenses involved and the necessity for substitutes such as biochar, there is a critical focus on investigating supplementary cementing materials (SCMs) to partially substitute traditional materials. The use of biochar as a concrete admixture is becoming more popular, and it has been investigated as a building material. Biochar is a solid organic residue produced by the pyrolysis of biomass. The experiment aimed to determine the mechanical characteristics of biochar-containing concrete using a concrete grade M20, cube moulds of dimension 100mm x 100mm x 100mm; cylinder moulds of 100mm x 200mm and beam formwork of dimension 150mm x 150mm x 1000mm were used to cast the control concrete sample and concrete containing varying percentages of biochar. Finite element analysis was also carried out using the ABAQUS program, utilizing concrete properties discovered through experimental study. The numerical and experimental study revealed that elevating the proportion of biochar in concrete led to about 17% decrease in compressive strength, 40% reduction in tensile strength, and about 25% reduction in the flexural strength of concrete beams. Both numerical and experimental approaches proved successful in assessing the influence of biochar on concrete.

Key words: Biochar, Compressive strength, Concrete, Flexural strength, Cement, Split tensile strength.

1. Introduction

The most used building material in the world is concrete, which is highly heterogeneous. The characteristics of the components used, the amount of the mix, the manner of compaction, and other controls due to the placement, compaction, and curing of the concrete are what give the concrete its strength, durability, and unique capabilities (Rashmi & Padmapriya, 2021). Cement emits 7% of global CO_2. Cement accounts for 90% of concrete's emissions. To enhance sustainability, use natural additives like rice husk ash, eggshells, waste materials (sludge, glass, foundry waste, tires), and biochar to boost concrete insulation and strength (Mensah et al., 2021). Biochar, a porous, stable, and carbon-rich material with high absorption and a basic pH, is used in agriculture to improve soil fertility, capture carbon, and mitigate climate change through long-term CO_2 sequestration (Cosentino et al., 2019). According to (Gupta, Kua, & Pang, 2018), Compared to carbon dioxide-saturated biochar, fresh biochar has greater mechanical strength and better permeability. Biochar can be explained to be the product of an organic substance that had undergone combustion under very minimal oxygen levels resulting in a carbon-rich material. Researchers at Politecnico di Torino have explored biochar's use as nano/microparticles in cement composites to enhance mechanical properties. Biochar serves as a non-reactive filler, improving durability by reducing porosity (Cosentino et al., 2019).

Flexural strength quantifies the amount of stress and forces an unreinforced concrete beam can sustain so that it can endure any bending failures (West, 1993). (Raheem et al., 2015) concluded that Cassava Peel Ash (CPA) replacement of 5%, 10%, and 15% showed no significant loss in strength compared to the control sample and is stable and could be acceptable in most

concrete.(Olatokunbo et al., 2018) conducted an experiment to ascertain the strength characteristics of CPA concrete by altering the percentages of CPA replacement for cement (5, 10, 15, 20 & 25 %) for 7, 14, 28, 90, 120, and 180 days. At 10% cement replacement with CPA, its durability and resistance to sulfuric acid significantly increased. The study suggests using CPA concrete for light building projects where longevity is a top priority but great strength is not a requirement.

Concrete's compressive strength is determined through a compression test, reflecting its ability to withstand compression forces. (Akhtar & Sarmah, 2018) investigated the compressive strength of biochar produced from three different feedstocks (poultry litter, rice husk, and pulp/paper mill sludge). Results showed biochar-added concrete had lower compressive strength than non-biochar-added concrete. (Ahmad et al., 2015) found that adding less biochar to the bamboo biochar cement composite increased compressive strength. Mrad (Mrad & Chehab, 2019) also observed a decrease in compressive strength when high percentages of biochar were used (5, 10, 15, 25, and 40 %).(Dixit et al., 2021) developed ultra-high performance concrete using biochar as a partial replacement material for quartz powder. After 28 days of curing, the strength of the 2% and 5% biochar concrete was reduced by about 13% and 14%, respectively, when compared to the non-biochar-added concrete. (Praneeth et al., 2020) explored the effect of replacing 10–40% of sand in concrete with biochar derived from poultry litter on compressive strength. The results indicated that the compressive strength of the samples decreased drastically with the addition of biochar. The inclusion of 0.5-0.8 percent hazelnut shell and coffee powder biochar resulted in a significant increase in compressive strength, as seen in the study of (Restuccia & Ferro, 2016). In the study observed by (Sirico et al., 2020), it was discovered that slight reduction of compressive strength at 7 and 28 days after the addition of 1 and 2.5% biochar from a mixture of woodchips of local forests (alder, beech, poplar, chestnut, oak, and hornbeam). (Gupta, Kua, & Low, 2018) reported an increase in compressive strength after the addition of up to 2% food waste and wood sawdust biochar.

Split tensile strength is the indirect method of determining the tensile strength of the concrete using a cylinder that splits across the vertical diameter (Bahij et al., 2020). (Gupta, Kua, & Pang, 2018) used biochar derived from mixed food waste, rice and wood waste as carbon sequestering additives in concrete, obtaining similar results in mechanical strength by adding 1–2 wt% of biochar compared to the control mix. Also, an increase of more than 20% in compressive and tensile strength was reached. (Akhtar & Sarmah, 2018) investigated the effect of biochar mixed with cement on the mechanical properties of concrete replacing the cement content of up to 1% of the total volume with three different types of biochar, such as poultry litter, rice husk, pulp, and paper mill sludge biochar. Results showed that compressive strength was almost equal to that of reference one by using pulp and paper mill sludge biochar at 0.1% replacement of total volume. (Asadi Zeidabadi et al., 2018) replaced a part of cement in a concrete mixture with rice husk and bagasse biochar. Concrete samples containing 5% biochar had a compressive and tensile strength improvement by more than 50% and 78% respectively, compared to ordinary mix.

Despite the valuable applications of cement, its production is a significant contributor to global CO_2 emissions, accounting for approximately 7%. The manufacturing of one tonne of cement results in the release of an equivalent amount of CO_2, as highlighted by (Mensah et al., 2021). This CO_2 emission poses environmental risks and negatively impacts the ecosystem. Additionally, the high cost associated with cement production presents another challenge that requires attention. Therefore, researching alternative materials, such as biochar, to partially replace cement with supplementary cementing materials (SCMs) is imperative. This study primarily assesses its suitability for structural applications by comparing concrete's mechanical properties with 2.5% and 5% biochar additions through experimental and numerical means.

2. Methodology

2.1. Procedure for Batching of concrete mix with biochar as an admixture

2.1.1. Materials

The cement used for the production of concrete is Portland Limestone Cement (PLC) Dangote 3x Cement Brand of grade 42.5N conforms to NIS 444-1:2018 CEM II/B-L 42.5N CB-4227. Clean water was obtained from a borehole at Kwara state University, Malete was used for the concrete; it was used for the concrete mix design. The fine aggregate used was obtained from Kwara State University as Natural sand that gathered as a result of erosion and passes through sieve 5.00 mm; while the coarse aggregate (crushed stones) maximum size of 20.00mm was used and both conforms to BS 882;1982. The cassava peel was obtained from Ganmo market in Kwara State through Mama Olupako and was dried up for one week as shown in Figure 1. The cassava peel was the biomass used which was converted to Biochar using a similar techniques by (Odeyemi et al., 2023) and (Adeniyi et al., 2023) . The cassava peel was burnt with the use of Reactor at Chemical engineering laboratory of University of Ilorin, Kwara State at a temperature of 600^{o}C for 2 hours which after then, it was allowed to cool and grind and them sieved through a 20μm sieve in order to remove the bigger sizes ash particles and impurities. Secondly, only fine bio char passes through 200μm was been used.

Fig. 1. Sun Drying of Cassava Peel

Dried sticks were used as the combustion fuel and kerosene was used to ignite in order to generate thermal energy. The name of the reactor used is called A top-lit fixed- bed updraft biomass resistance. The inner chamber which contained the biomass is called carbonization chamber. A CASON CA380 infrared thermometer was used for temperature monitoring. The triangular hole at the outer reactor (bottom) is to allow the updraft of oxygen to the combustion front at the top of the reactor. The reactor operates on a top-lit updraft configuration 'Top-lit' signifies that the combustion fuel is ignited at the top and burns gradually downwards until all of the fuel is consumed, Figure 2 shows how a top-lit fixed-bed updraft biomass reactance was being process. Updraft signifies that the air flow is usually by diffusion through the bottom air holes in an upward direction to the combustion front. The heating system uses retort heating. The biomass fuel is utilized or recycled as the heat source in converting the biomass in the inner chamber. The essence of air holes present on the sides of the inner chamber is to prevent the pyrolysis of the biomass.

Fig. 2. A top-lit fixed-bed updraft biomass reactance

2.1.2. Preparation of test specimens

Concrete cube moulds of 100mm x 100mm x 100mm were used to cast concrete for the compressive strength test, and cylinder moulds of dimensions 100mm x 200mm were utilized as well to cast concrete for the split tensile strength test. Individually, the moulds were meticulously oiled prior to the casting of concrete in them. The freshly mixed concrete mix were placed in layers of three in each of the moulds, for each layer effective compaction was done with the aid of a compaction rod, about 25 strokes was applied to reduce the possibility of the presence of voids as recommended by the British Standard codes BS 12390 Part 2 (BSI, 2019). The concrete surface was subsequently levelled. A concrete mix ratio of 1:2:4 was used for the M20 concrete, biochar was introduced by percentage weight of cement into the mix at 2.5% and the samples were cured for 7, 28 and 56 days. For the flexural strength test, the concrete mix was meticulously cast into the beam mould of dimensions 150mm width, 150mm depth and 1000mm length, two samples were also produced for the concrete control sample and 2.5% by weight of cement in concrete.

2.2. Abaqus Software

Abaqus FEA is a comprehensive software package designed for analyzing finite elements and assisting in computer-aided engineering tasks. It provides a smooth integration of Dynamic-Static co-simulation capabilities, allowing users to seamlessly switch between implicit and explicit solvers for highway dynamics. The software incorporates a concrete damaged plasticity model, specifically designed to accurately represent the behavior of materials that exhibit quasi-brittle characteristics. This model utilizes both isotropic damaged elasticity and isotropic tensile and compressive plasticity. Abaqus FEA is capable of simulating plain concrete and reinforced concrete structures, and it supports the inclusion of reinforcement modeling using rebar. Additionally, the software grants users control over stiffness recovery effects, demonstrates sensitivity to straining rates, and offers the option to incorporate viscoelastic regularization, which enhances convergence rates when dealing with softening behaviors. The commercial software ABAQUS Standard 6.13 was utilized to perform numerical simulations of M20 concrete material.

2.3. Numerical analysis of the compressive strength test

Concrete Damaged Plasticity is a well-established and practical constitutive model widely acknowledged for accurately simulating concrete behaviour. The model's parameters concerning relative concrete damage under compression and tension were determined by correlating stress-strain relationships obtained from experimental studies involving uniaxial compression and tension loading. These stress-strain relationships were derived from the experimental work in this study and (Wahalathantri et al., 2008). Other parameters that could not be obtained experimentally were assumed based on parameters of normal-strength concrete. The formulae

used in computing the damage parameters were gotten from (Al-Rifaie & Mohammed, 2022). The formulae for the inelastic and damaged parameters are given in Eq. 1 and Eq. 2 respectively.

$$\varepsilon^{in} = \varepsilon - \varepsilon^{el}; \quad (1)$$

where $\varepsilon = strain,\ \varepsilon^{el} = elastic\ strain$

$$d = 1 - \frac{\sigma}{\sigma_c}; \quad (2)$$

where $\sigma_c = stress\ at\ peak,\ \sigma = stress$

2.3.1. Materials properties

Table 1 shows the properties of M20 Concrete. The density of concrete used was 2433kg/m^3 and the young modulus E was 52.57N/mm^2 (Adegoke et al., 2022). The dilation angle, eccentricity, initial biaxial/uniaxial ratio, and k used for the analysis of 0% and 2.5% of biochar are shown in Table 2.

Table 1. Properties of M20 Concrete

PARAMETERS	Value
Dilation angle	40
Uniaxial/Biaxial ratio ($\mathcal{E}_{co}$ /$\mathcal{E}_{b0}$)	1.16
Eccentricity	0.1
Viscosity parameter	0
Poisson ratio	0.2
The shape of the loading surface (K)	0.667

Table 2. Material property parameters for 0 and 2.5% of biochar

Dilation angle	40
Eccentricity	0.1
Initial biaxial / uniaxial ratio	1.16
k	0.667
Viscosity parameter	0

The Young's modulus and the density for the control samples at 0% biochar are 200.76 N/mm^2 and 2430 kg/m^3 respectively. Young's modulus and density for concrete with 2.5% biochar are 248.18 N/mm^2 and 2348 kg/m^3 respectively. Young's modulus and density were gotten from the experimental test carried out in this study. Table 3 displays the experiment characteristics of biochar, focusing on its physical properties.

Table 3. Physical properties of Biochar for the experiment

Property	Result	Standards used
Density	0.230 g/cm^3	IBI (IBI, 2013)
pH	7	IBI (IBI, 2013)
Particle Size	90 micrometers	BS EN 933-1 (BS EN 933-2:2020 Tests for Geometrical Properties of Aggregates - Part 2: Determination of Size Distribution - Test Sieves, Nominal Size of Apertures, 2020)
Water absorption test	4.6%	IBI [22]
Initial setting time (2.5% biochar + Cement)	42 min	BS EN 196-3 (BS EN 196-3, 2016)
Final setting time (2.5% biochar + cement)	513 min	BS EN 196-3 (BS EN 196-3, 2016)

*The comprehensive datasets used in the constitutive model are available on request

2.3.2. Modules

Abaqus/CAE is divided into modules, where each module defines an aspect of the modeling and analysis process. They are Part Module, Property module, Assembly Module, Step module, Interaction, Load, Mesh, job, and Visualization. The model used in this study is a cube with a geometry of 100mm in depth, 100mm in breadth, and 100mm in height. A rigid body plate of 150mm diameter was also modeled to apply the pressure properly on the modelled concrete cube. As illustrated in Figure 3(a) and (b).

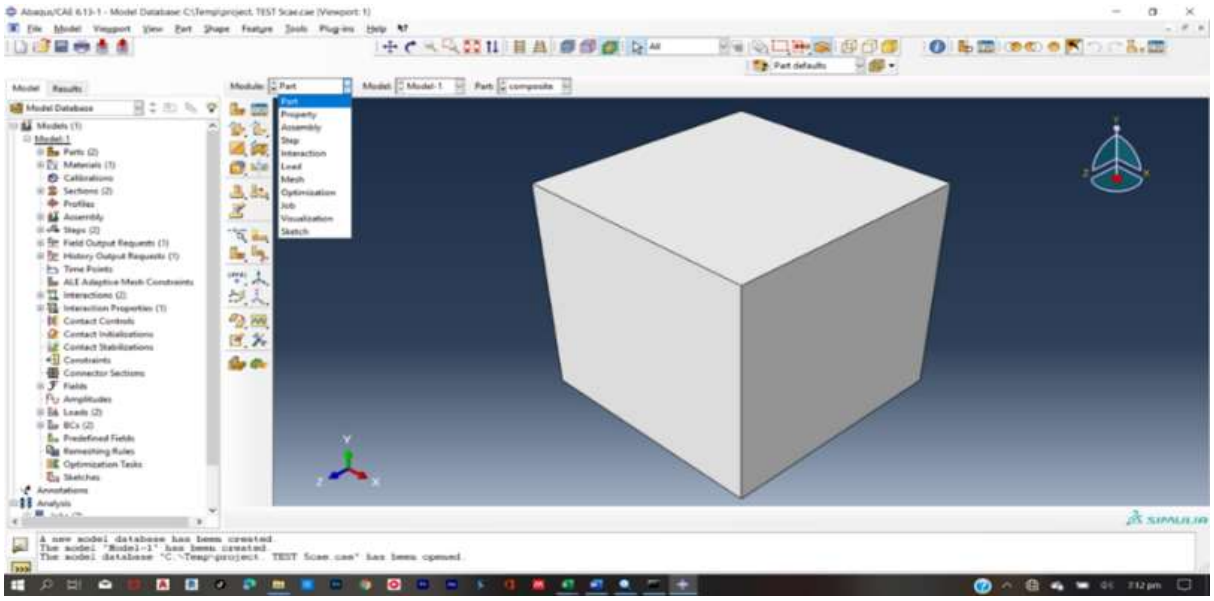

(a)

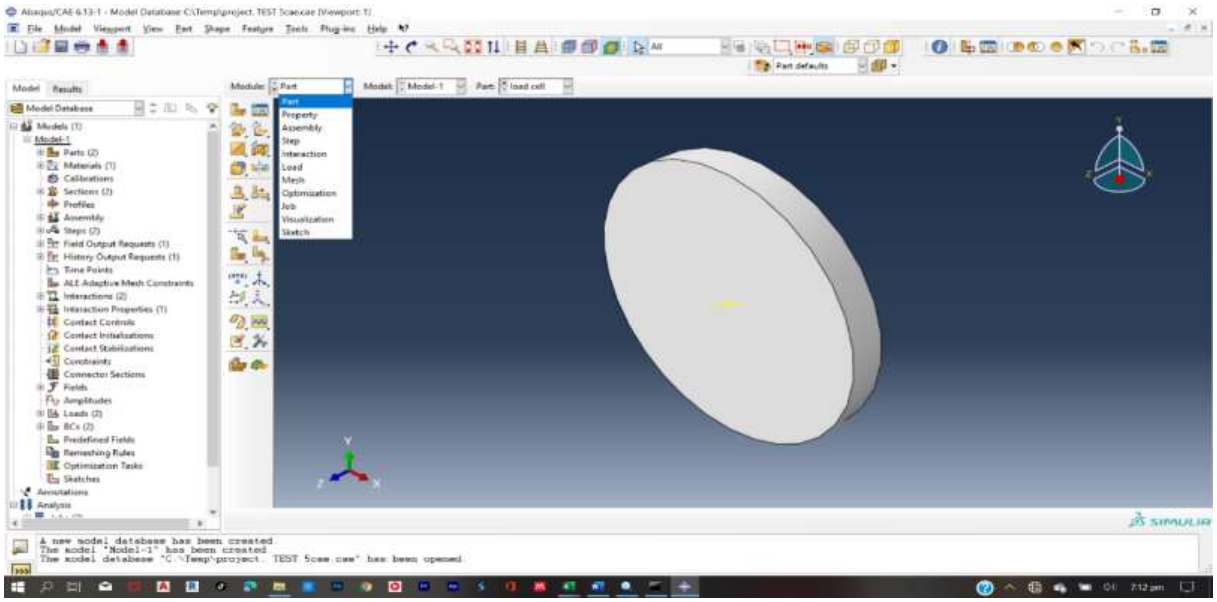

(b)

Fig. 3. ABAQUS Part module (a) cube (b) plate

Figure 4 shows the property module, the section properties were added, such as the density, the elastic properties, and the concrete damaged plasticity properties, and inelastic strain properties were assigned to the sections created in the part region.

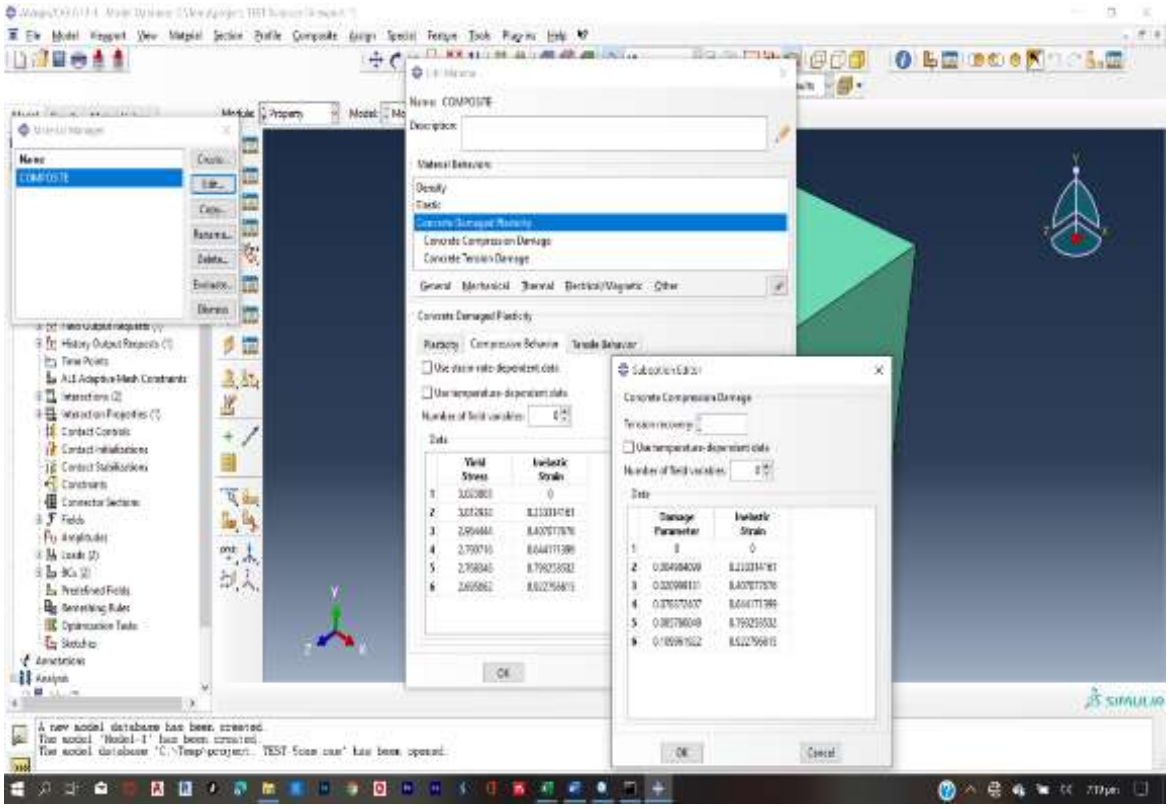

Fig. 4. Property module showing the material properties (Damage parameters)

The ABAQUS software was used to create a model consisting of a single assembly, enabling the combination of various parts into one model. The rigid body plates were fixed at both ends of the cube, as illustrated in Figure 5. The step sequence feature was employed to capture model changes, such as variations in loading and boundary conditions. Output requests could be adjusted as needed for each step. The interaction module facilitated the definition of mechanical and thermal interactions between surfaces, including contact and friction coefficients. This module allowed for the specification of load and boundary conditions.

Within the mesh module, tools were available to generate a finite element mesh for the assembled components in ABAQUS/CAE. Once all the necessary model definitions were completed, this module was used to analyze the model. It provided the capability to interactively submit analysis tasks and monitor their results. The load module, depicted in Figure 6, facilitated the definition of load and boundary conditions. The visualization module offered a graphical display of the finite element models and their results. Figure 7 presented the Von Mises stress distribution up to its maximum value.

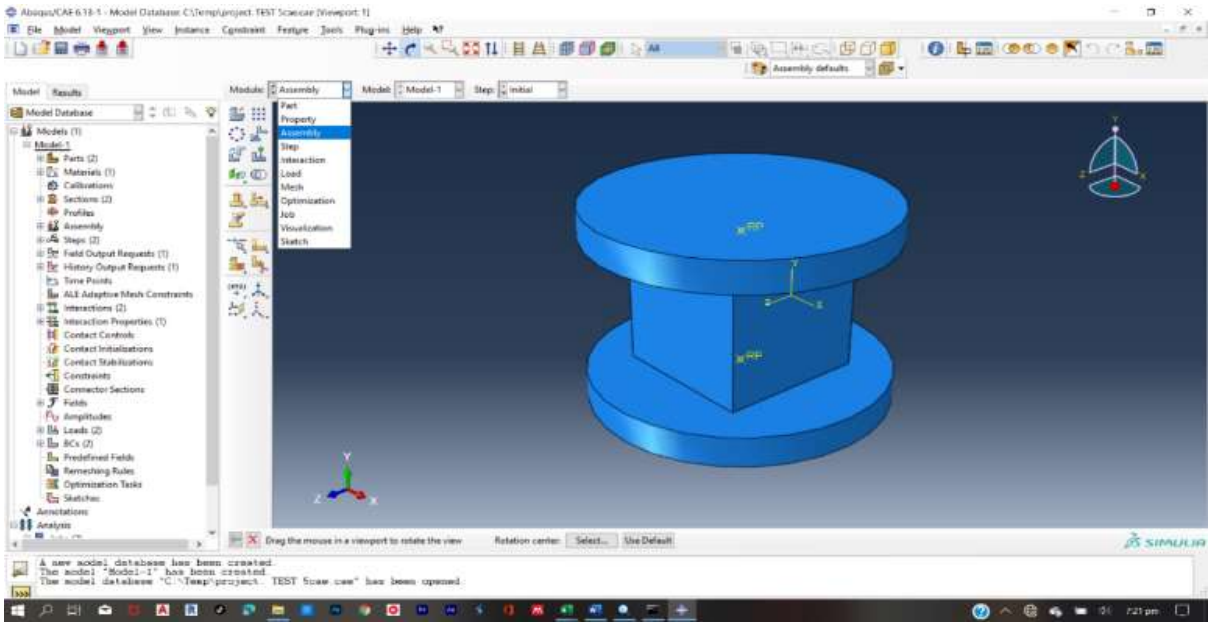

Fig. 5. Assembly module showing the assemblage of the cube and the plates

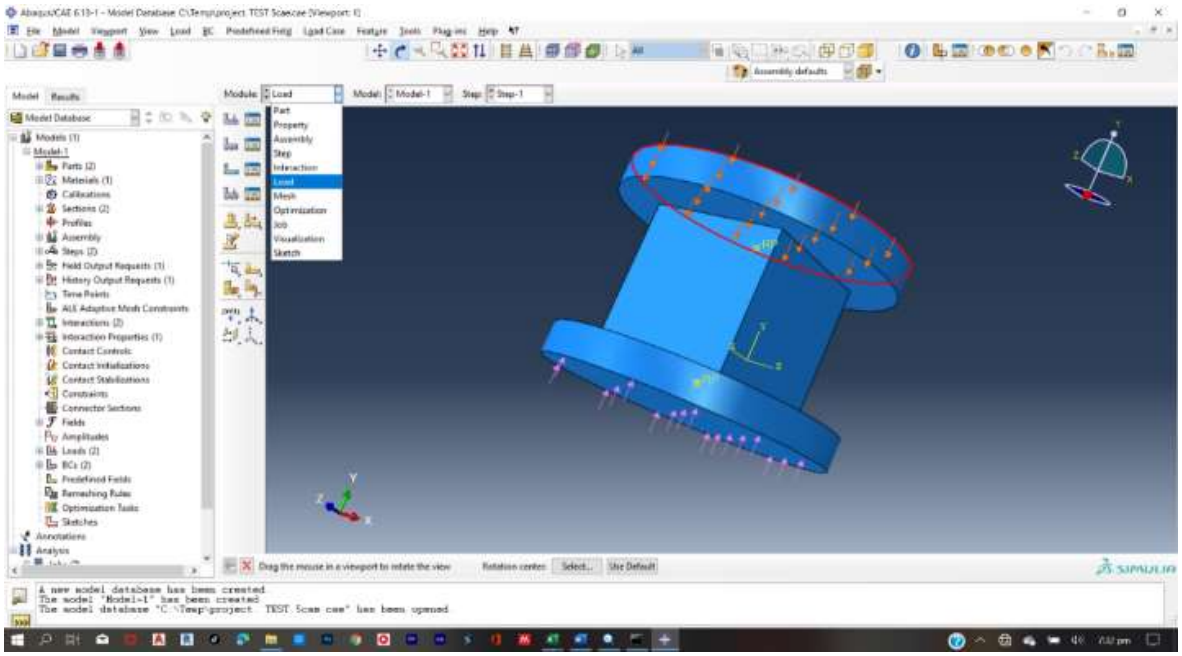

Fig. 6. Load module showing the module required to crush the cube

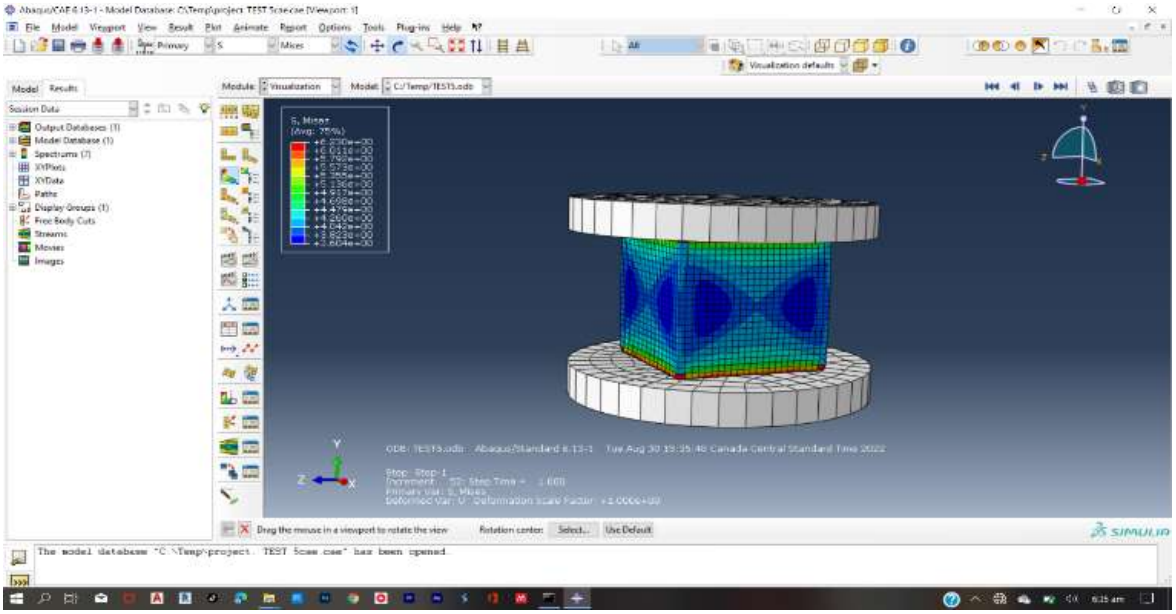

Fig. 7. Visualization module showing the extent of crushing

2.3.3. Tensile strength test

A model database was generated, and the part module was employed to define the geometry of the concrete cylinder as a deformable solid and the sprite as a discrete rigid shell. The extrusion form was used for both, with approximate dimensions of (100mm x 200mm) for the concrete cylinder and (10mm x 30mm x 200mm) for the sprit (BS EN 12390-6, 2011). Figure 8(a) and (b) depicts the modelled cylinder and strut.

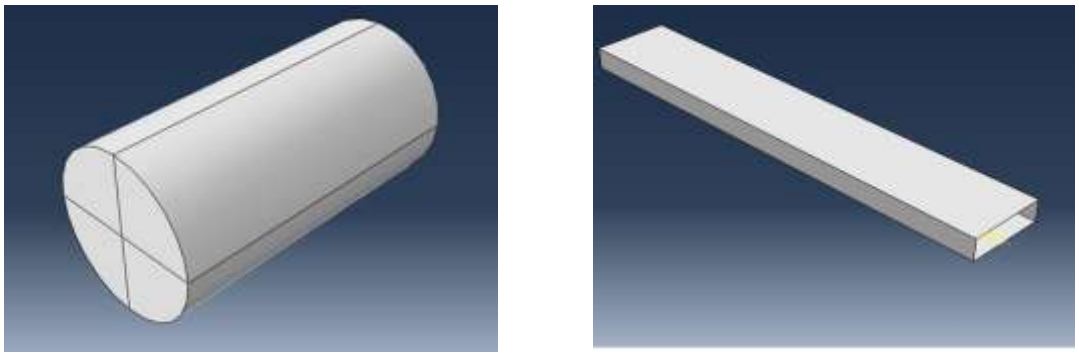

(a) **(b)**

Fig. 8. (a) Concrete cylinder part (b) Sprit part

Instances were generated to create a pattern of the dependent part, incorporating both the concrete cylinder and sprite, as illustrated in Figure 8. Field output was established to capture force or reaction (static, general), and specific boundary conditions were defined. The seed part instance was chosen, and a global size of approximately 6 was applied for mesh generation, utilizing the selected mesh part instance, as depicted in Figure 9 and Figure 10. A split tensile test configuration was established, with default settings for all other options, and the analysis was subsequently initiated.

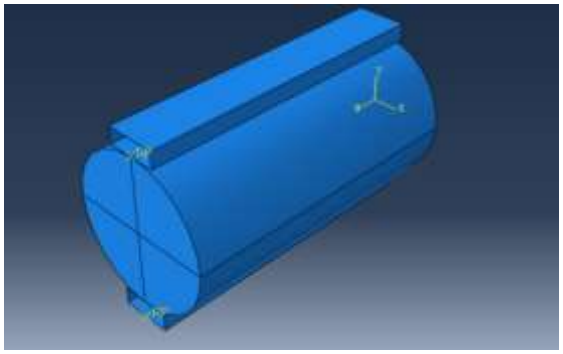

Fig. 9. Assembly of concrete and sprite

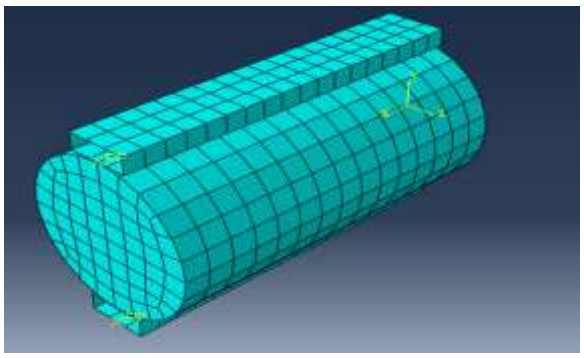

Fig. 10. Independent mesh part

2.3.4. Flexural strength Test

The part for the beam was created and the size of the beam to be modeled was 1000mm x 150mm x 150mm (British Standards, 2009). The partitions for the supports and the load on the beam was created since the beam was modeled using a three-point loading as illustrated in Figure 11. The parts for the supports were also created. The material properties defined were assigned to each material. The section type assigned to the beam model was solid, homogenous. The step type was defined to be dynamic, explicit and the field output was created. Interaction contact property options were chosen, the tangential behavior and the normal behavior were defined. The load type which is the point load was applied directly on the beam and the boundary conditions were defined for U_1, U_2 and U_3. The seed part instance was selected and an approximate global size of 6 was used for the meshing, the mesh part was selected to generate the meshes as depicted in Figure 12. The job name for the analysis was created and the data was checked for the analysis.

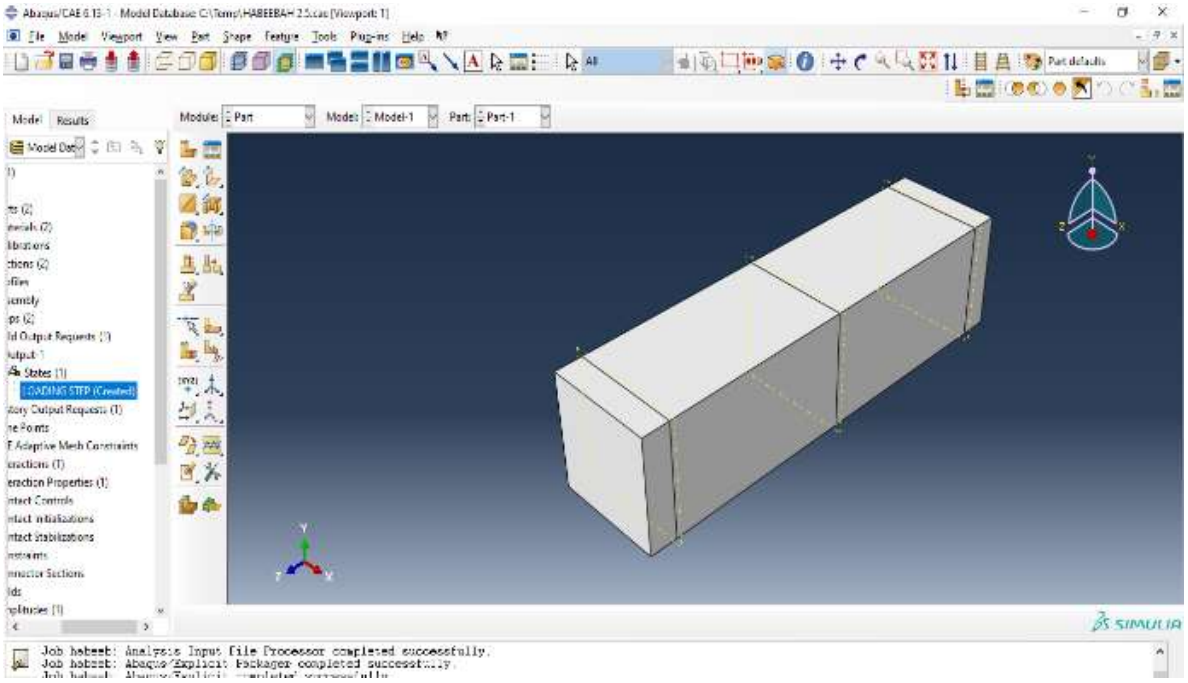

Fig. 11. Beam model and partitions

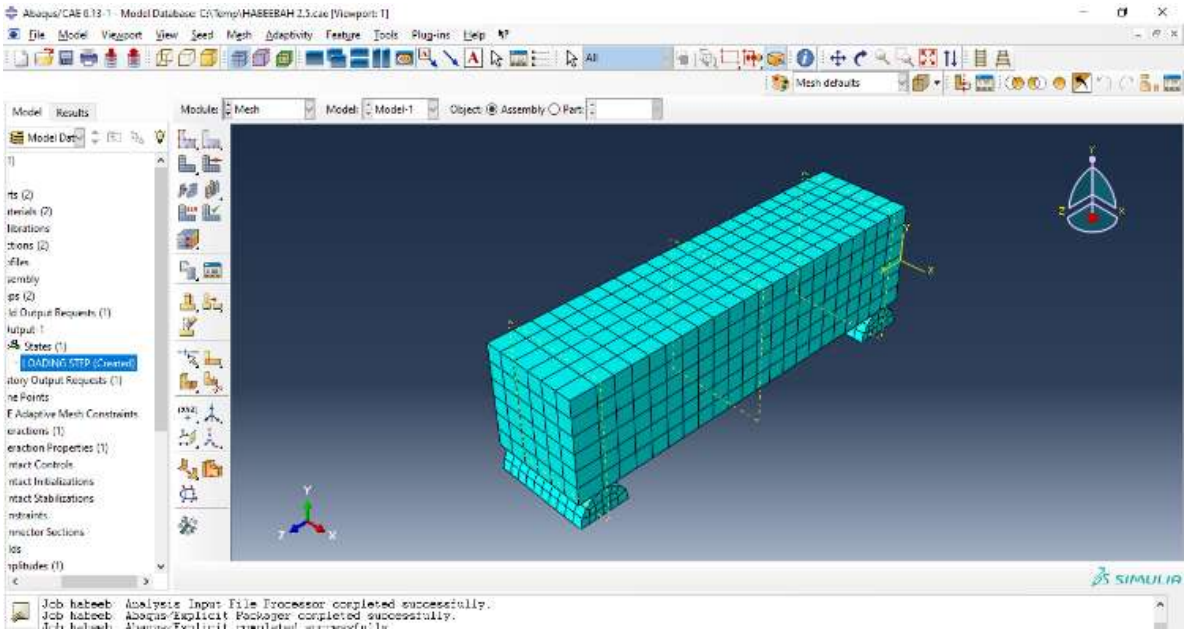

Fig. 12. Meshing of the beam model

3. Results and discussion

3.1. Compressive Strength Results

3.1.1. Stress Distribution

Figure 13 and Figure 14 shows the stress distribution for the control sample and the sample at 2.5% biochar respectively. Figure 15 depicts the numerical compressive strength of concrete with varying percentages of biochar.

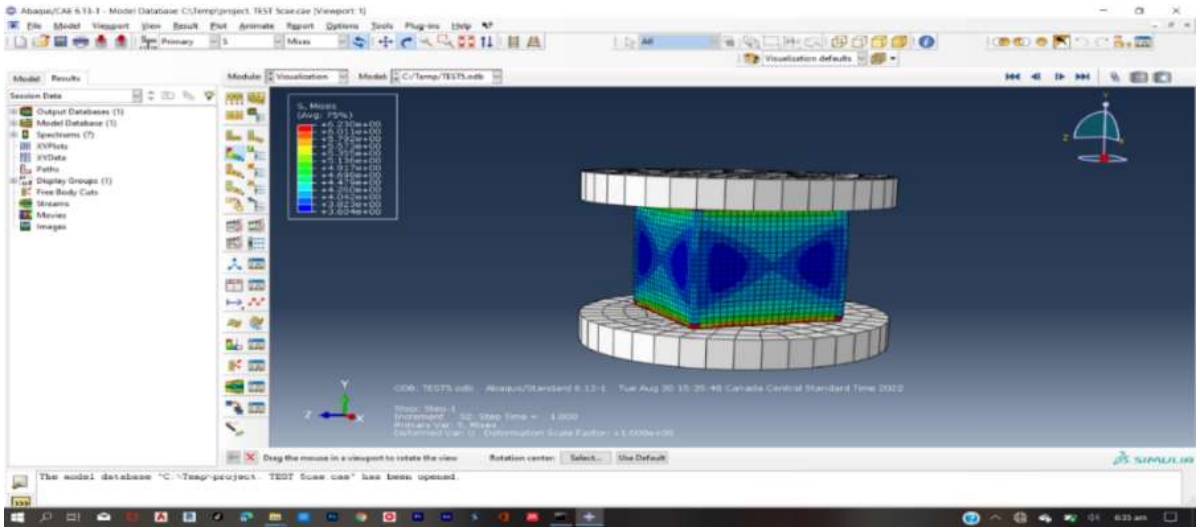

Fig. 13. Stress distribution result of 0% of replacement with biochar

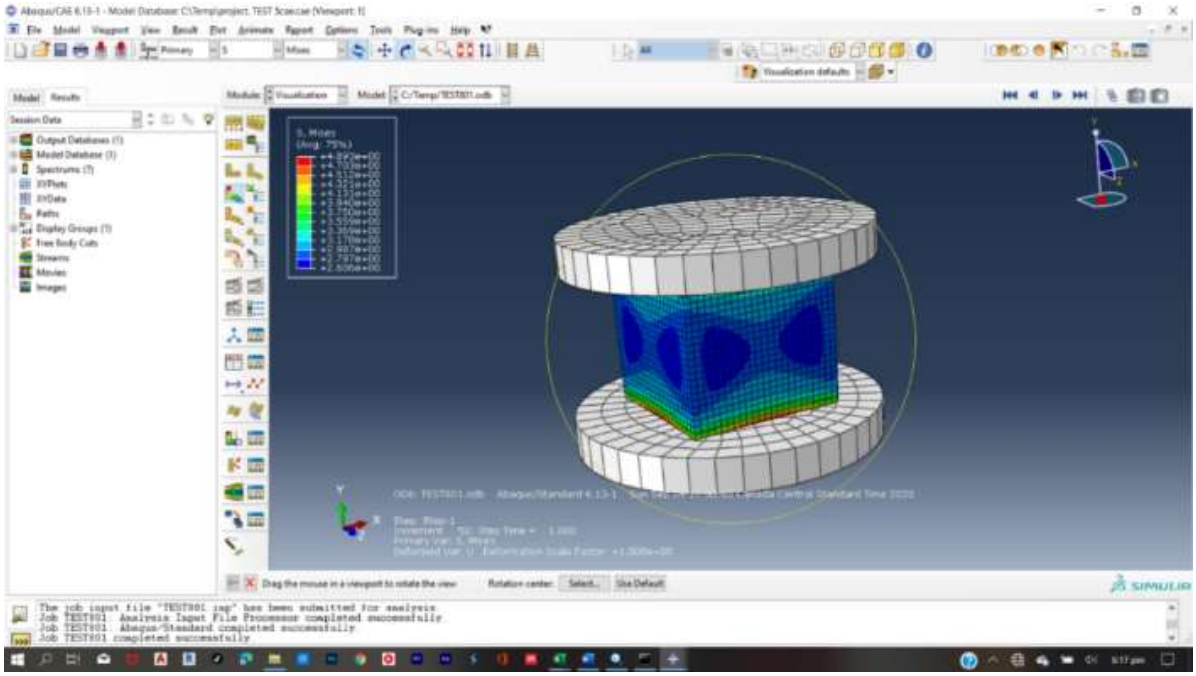

Fig. 14. Stress distribution result of 2.5% of replacement with biochar

The graphical representation in Figure 15 reveals that the outcome of the experimental results surpassed the numerical results. This disparity can be attributed to constraints inherent in the numerical analysis. According to the numerical tests, the concrete without biochar exhibited a compressive strength of 23.15 N/mm^2, surpassing the 19.21 N/mm^2 exhibited by the concrete with 2.5% biochar. A similar pattern is evident in the experimental tests, where the control concrete and the concrete with 2.5% biochar demonstrated compressive strengths of 24.54 N/mm^2 and 20.13 N/mm^2, respectively after a 56-day curing period. The dominance of the weakening effects was observed when the biochar content exceeded 0%, which aligns with earlier studies (Maljaee et al., 2021)(Gupta, Kua, & Koh, 2018).

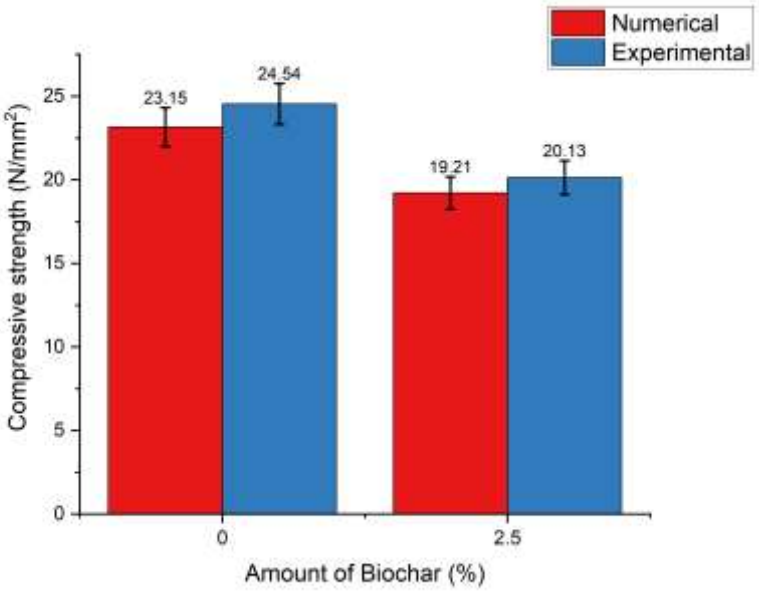

Fig. 15. Compressive strength of concrete with varying percentages of biochar by experimental and numerical tests

3.2. Split Tensile Strength Result

3.2.1. Stress Distribution

The stress distribution of the control sample at 0% and concrete with 2.5% biochar is presented in Figure 16 and Figure 17 respectively.

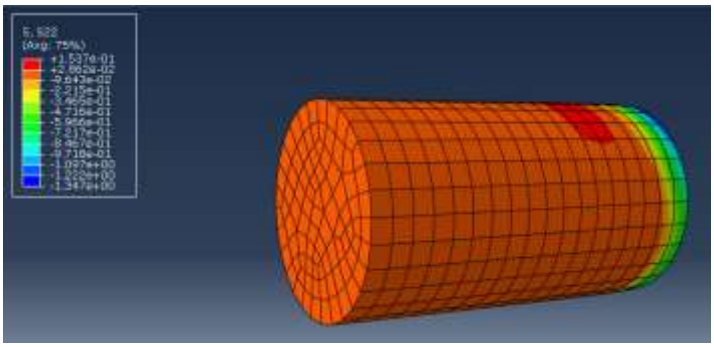

Fig. 16. Stress distribution of concrete containing 0% of biochar

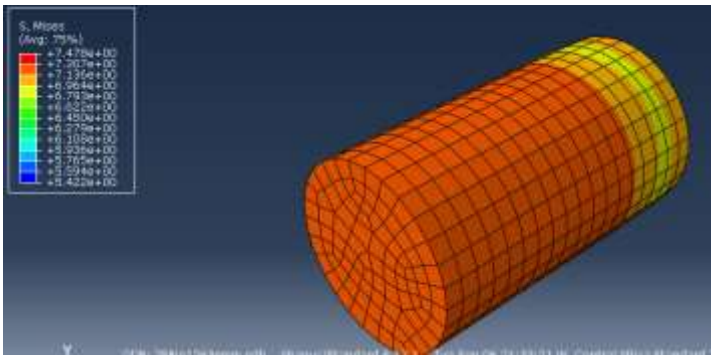

Fig. 17. Stress distribution of concrete containing 2.5% of biochar

The split tensile results are illustrated in Figure 18. In the numerical analysis, the maximum tensile strength recorded was 3.01 N/mm^2 for concrete with 2.5% biochar and 5.37 N/mm^2 for the control sample, as depicted in Figure 18. Contrarily, the experimental tests conducted after 56 days revealed a split tensile strength of 4.67 N/mm^2 for the control sample and 2.92 N/mm^2 for the sample with 2.5% biochar. Generally, the biochar reduces the split tensile strength of concrete. It is noteworthy that the numerical results surpass the experimental results, potentially attributable to environmental influences.

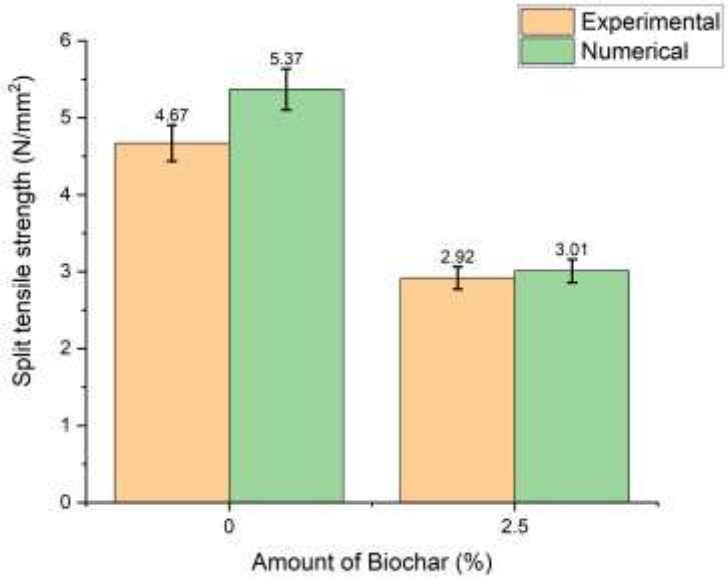

Fig. 18. Tensile strength of concrete with varying percentages of biochar by experimental and numerical tests

3.3. Flexural strength result

3.3.1. Stress Distribution

The deflection results of control sample and concrete containing 2.5% biochar are displayed in Figure 19 and Figure 20 respectively.

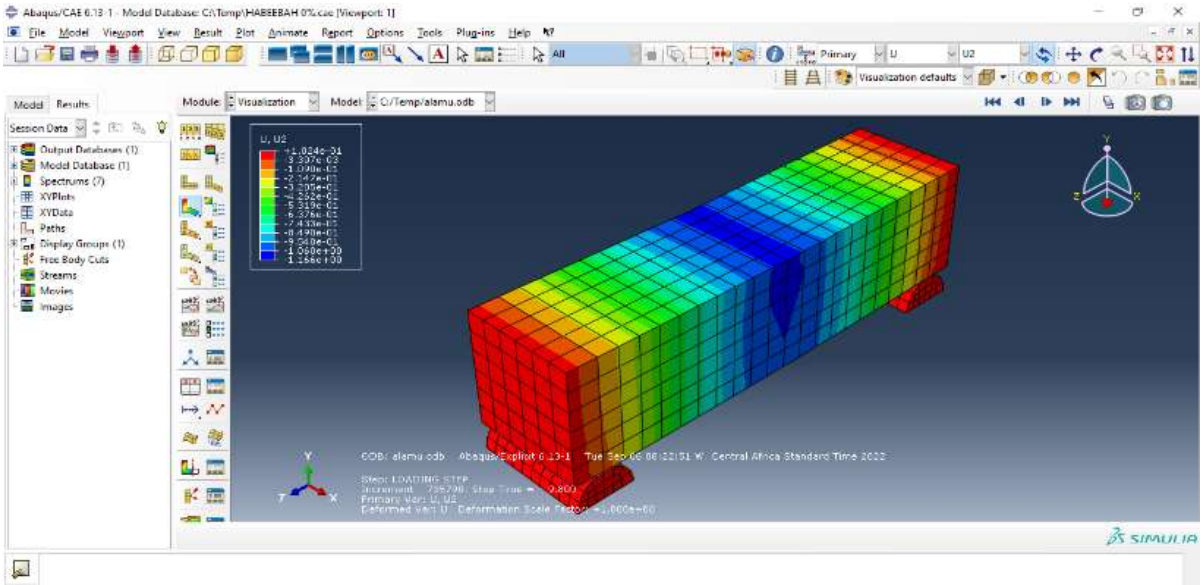

Fig. 19. Deflection of control sample

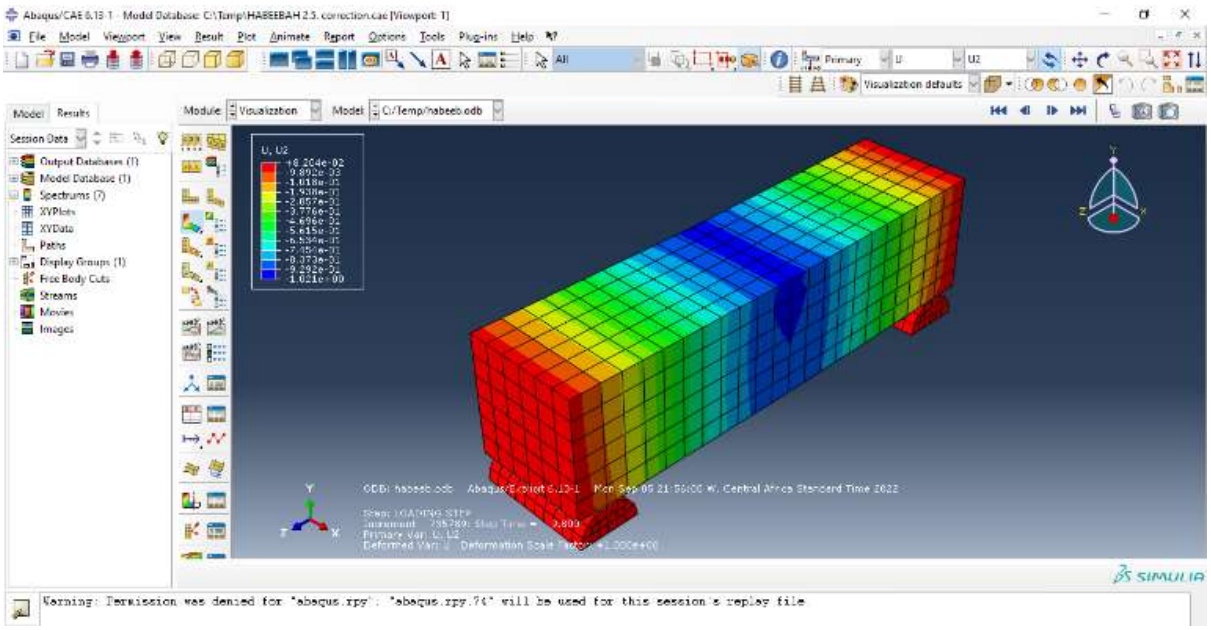

Fig. 20. Deflection of concrete containing 2.5% of biochar

Figure 21 displays the ultimate load values for concrete samples. In the numerical findings, the control sample exhibited a maximum failure load of 4.4 KN, while the sample with 2.5% biochar had a maximum analytically determined failure load of 3.4 KN. Experimental results from the flexural strength test on concrete beams, conducted after 56 days, revealed ultimate load values of 3.6 KN and 2.5 KN for the 0% and 2.5% biochar samples, respectively. The numerical values surpass the experimental results, possibly due to limitations in the ability of numerical models to accurately depict the actual behavior of concrete when subjected to flexural load.

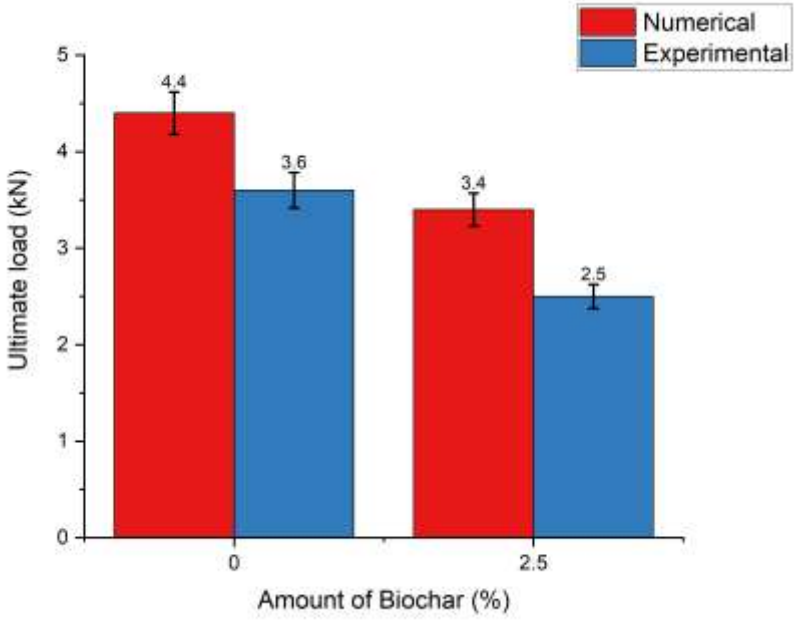

Fig. 21. Ultimate load of concrete with varying percentages of biochar by experimental and numerical tests

4. Conclusion

This research examines the impact of incorporating biochar into low-cost, low-carbon concrete and evaluates its mechanical performance using both finite element analysis and experimental. Based on the conducted analysis, the following conclusions can be derived from the aforementioned investigations.

1. Increasing the biochar content in the concrete led to a reduction in compressive strength.
2. The inclusion of biochar resulted in a decrease in tensile strength compared to concrete without biochar.
3. Biochar decreases the flexural strength of concrete.
4. The increase in dosage of biochar increases the deflection of concrete beam.
5. Both numerical and experimental methods were efficient to determine the impact of biochar in concrete

5. References

Adegoke, M., Shokouhian, M., & Ntonifor, C. (2022). AFRP Reinforced Concrete Column with Controlled Rocking Connection. *Structures Congress 2022 - Selected Papers from the Structures Congress 2022*. https://doi.org/10.1061/9780784484180.010

Adeniyi, A. G., Adeyanju, C. A., Iwuozor, K. O., Odeyemi, S. O., Emenike, E. C., Ogunniyi, S., & Te-Erebe, D. K. (2023). Retort carbonization of bamboo (Bambusa vulgaris) waste for thermal energy recovery. *Clean Technologies and Environmental Policy*, *25*(3). https://doi.org/10.1007/s10098-022-02415-w

Ahmad, S., Khushnood, R. A., Jagdale, P., Tulliani, J. M., & Ferro, G. A. (2015). High performance self-consolidating cementitious composites by using micro carbonized bamboo particles. *Materials & Design*, *76*, 223–229. https://doi.org/10.1016/J.MATDES.2015.03.048

Akhtar, A., & Sarmah, A. K. (2018). Novel biochar-concrete composites: Manufacturing, characterization and evaluation of the mechanical properties. *Science of The Total Environment*, *616–617*, 408–416. https://doi.org/10.1016/J.SCITOTENV.2017.10.319

Al-Rifaie, H., & Mohammed, D. (2022). Comparative Assessment of Commonly Used Concrete Damage Plasticity Material Parameters. *Engineering Transactions*, *70*(2). https://doi.org/10.24423/EngTrans.1645.20220613

Asadi Zeidabadi, Z., Bakhtiari, S., Abbaslou, H., & Ghanizadeh, A. R. (2018). Synthesis, characterization and evaluation of biochar from agricultural waste biomass for use in building materials. *Construction and Building Materials*, *181*. https://doi.org/10.1016/j.conbuildmat.2018.05.271

Bahij, S., Omary, S., Feugeas, F., & Faqiri, A. (2020). Fresh and hardened properties of concrete containing different forms of plastic waste – A review. In *Waste Management* (Vol. 113). https://doi.org/10.1016/j.wasman.2020.05.048

British Standards. (2009). BS EN 12390-5 - Flexural Strength of Test Specimens. In *British Standard Institutes* (Vol. 37).

BS EN 12390-6. (2011). Tensile splitting strength of test specimens. *BSI Standards*, *3*(1).

BS EN 196-3. (2016). Methods of testing cement -– Part 3: determination of setting times and soundness. *British Standard*.

BSI. (2019). BS EN 12390-2:2019 Testing hardened concrete. Part 2: Making and curing specimens for strength tests. *BSI Standards Publication*.

BS EN 933-2:2020 Tests for geometrical properties of aggregates - part 2: Determination of size distribution - Test sieves, nominal size of apertures, British Standard (2020).

Cosentino, I., Restuccia, L., Ferro, G. A., & Tulliani, J. M. (2019). Type of materials, pyrolysis conditions, carbon content and size dimensions: The parameters that influence the mechanical properties of biochar cement-based composites. *Theoretical and Applied Fracture Mechanics*, *103*. https://doi.org/10.1016/j.tafmec.2019.102261

Dixit, A., Verma, A., & Pang, S. D. (2021). Dual waste utilization in ultra-high performance concrete using biochar and marine clay. *Cement and Concrete Composites*, *120*. https://doi.org/10.1016/j.cemconcomp.2021.104049

Gupta, S., Kua, H. W., & Koh, H. J. (2018). Application of biochar from food and wood waste as green admixture for cement mortar. *Science of the Total Environment*, *619–620*. https://doi.org/10.1016/j.scitotenv.2017.11.044

Gupta, S., Kua, H. W., & Low, C. Y. (2018). Use of biochar as carbon sequestering additive in cement mortar. *Cement and Concrete Composites*, *87*. https://doi.org/10.1016/j.cemconcomp.2017.12.009

Gupta, S., Kua, H. W., & Pang, S. D. (2018). Biochar-mortar composite: Manufacturing, evaluation of physical properties and economic viability. *Construction and Building Materials*, *167*. https://doi.org/10.1016/j.conbuildmat.2018.02.104

IBI. (2013). Standardized Product Definition and Product Testing Guidelines for Biochar that is Used in Soil | International Biochar Initiative. *Ibi*, *April*.

Maljaee, H., Madadi, R., Paiva, H., Tarelho, L., & Ferreira, V. M. (2021). Incorporation of biochar in cementitious materials: A roadmap of biochar selection. In *Construction and Building Materials* (Vol. 283). https://doi.org/10.1016/j.conbuildmat.2021.122757

Mensah, R. A., Shanmugam, V., Narayanan, S., Razavi, S. M. J., Ulfberg, A., Blanksvärd, T., Sayahi, F., Simonsson, P., Reinke, B., Försth, M., Sas, G., Sas, D., & Das, O. (2021). Biochar-added cementitious materials—a review on mechanical, thermal, and environmental properties. *Sustainability (Switzerland)*, *13*(16). https://doi.org/10.3390/su13169336

Mrad, R., & Chehab, G. (2019). Mechanical and Microstructure Properties of Biochar-Based Mortar: An Internal Curing Agent for PCC. *Sustainability 2019, Vol. 11, Page 2491*, *11*(9), 2491. https://doi.org/10.3390/SU11092491

Odeyemi, S. O., Iwuozor, K. O., Emenike, E. C., Odeyemi, O. T., & Adeniyi, A. G. (2023). Valorization of waste cassava peel into biochar: An alternative to electrically-powered process. *Total Environment Research Themes*, *6*. https://doi.org/10.1016/j.totert.2023.100029

Olatokunbo, O., Ede, A. N., Rotimi, O., Solomon, O., Tolulope, A., John, O., & Adeoye, O. (2018). Assessment of strength properties of cassava peel ash-concrete. *International Journal of Civil Engineering and Technology*, *9*(1), 965–974.

Praneeth, S., Guo, R., Wang, T., Dubey, B. K., & Sarmah, A. K. (2020). Accelerated carbonation of biochar reinforced cement-fly ash composites: Enhancing and sequestering CO2 in building materials. *Construction and Building Materials*, *244*. https://doi.org/10.1016/j.conbuildmat.2020.118363

Raheem, Arubike, E. D., & Awogboro, O. S. (2015). Effects of Cassava Peel Ash (CPA) as Alternative Binder in Concrete. *International Journal of Constructive Research in Civil Engineering*, *1*(2).

Rashmi, R., & Padmapriya, R. (2021). Experimental and analytical study on flexural behavior of reinforced concrete beams using nano silica. *Materials Today: Proceedings*, *50*. https://doi.org/10.1016/j.matpr.2021.04.127

Restuccia, L., & Ferro, G. A. (2016). Promising low cost carbon-based materials to improve strength and toughness in cement composites. *Construction and Building Materials*, *126*.

https://doi.org/10.1016/j.conbuildmat.2016.09.101

Sirico, A., Bernardi, P., Belletti, B., Malcevschi, A., Dalcanale, E., Domenichelli, I., Fornoni, P., & Moretti, E. (2020). Mechanical characterization of cement-based materials containing biochar from gasification. *Construction and Building Materials*, *246*. https://doi.org/10.1016/j.conbuildmat.2020.118490

Wahalathantri, B. L., Chan, T. H. T., & Fawzia, &. (2008). A Material Model for Flexural Crack Simulation in Reinforced Concrete Elements Using Abaqus Wahalathantri,. *Proceedings of the First International Conference on Engineering, Designing and Developing the Built Environment for Sustainable Wellbeing*.

West, H. H. (1993). Fundamentals of Structural Analysis. *European Journal of Engineering Education*, *18*(2). https://doi.org/10.1080/03043799308928177